

Spectral frustration and spatial coherence in thermal near-field spectroscopy

Brian T. O'Callahan, William E. Lewis, Andrew C. Jones, and Markus B. Raschke*

Department of Physics, Department of Chemistry, and JILA, University of Colorado, Boulder, Colorado 80309, USA

(Received 28 January 2014; revised manuscript received 29 May 2014; published 30 June 2014)

Scattering scanning near-field microscopy recently provided spectroscopic access to the fundamentally distinct spatial, spectral, and coherence properties of the thermal near field. Using SiC as an example, we study its thermal surface phonon polariton (SPhP) response. In contrast to the strongly surface-confined thermal near field of localized vibrational modes, an extended exponential distance dependence is observed reflecting the spatial coherence of the SPhP thermal field. In addition, we observe pronounced spectral frustration with spectral shifts ranging from ~ 5 to ~ 50 cm^{-1} that cannot be explained by conventional tip-sample dipole coupling alone. We present an alternative model describing an effective medium change by the tip. The results highlight the possibility for local spectral and spatial tuning of the thermal SPhP resonance for control of the light-matter interaction using thermal near-field radiation.

DOI: [10.1103/PhysRevB.89.245446](https://doi.org/10.1103/PhysRevB.89.245446)

PACS number(s): 68.37.Uv, 44.40.+a, 65.40.gp

I. INTRODUCTION

Emission of thermal radiation is a universal phenomenon. Its far-field behavior is described by Planck's law for the ideal blackbody, and its spectral modification for real ("gray") media is well understood. Of the associated evanescent *thermal near field* in close proximity to the emitter, a wide range of fundamentally distinct spectral, spatial, resonant, and coherence properties have been identified [1,2]. Their properties gained recent attention for enhanced nanoscale heat transfer [3] and broadband chemical nanospectroscopy [4] and fundamentally relate to the Casimir and Casimir-Polder forces [5].

The origin of thermal radiation is in transient excitations of charge carriers due to thermal fluctuations. The thermal near field is resonantly enhanced by electronic or lattice, collective, or single-particle resonances. Of particular recent interest is the ability enabled by new scanning probe microscopies [3,5], e.g., in the form of thermal radiation scanning tunneling microscopy (TR-STM) [6] or thermal infrared near-field spectroscopy (TINS) [4,7] for the spectral, spatial, or coherence characterization of the thermal near field.

However, TR-STM and TINS rely on the frustration of the evanescent field through scattering by a nanoparticle or the apex of a scanning probe tip. This raises the question of the degree of perturbation and thus relationship of the measured signal to the unperturbed electromagnetic local density of states (EM-LDOS). Using TINS, a generally good agreement has been found between experiment and theoretical resonant EM-LDOS peak positions and linewidths of both intrinsic molecular resonances, as well as for weak extrinsic surface phonon polariton (SPhP) resonances of SiO_2 [4]. However, recent TR-STM spectroscopy on SiC found a large ~ 40 cm^{-1} redshift and significant broadening of the SPhP resonance [7]. This effect was attributed to tip-sample coupling, but modeling the tip as a spherical scatterer required the assumption of a $1.6\text{-}\mu\text{m}$ tip apex radius which is 1–2 orders of magnitude larger than the actual tip radius [7].

Here we investigate the perturbation of both the spectral and spatial characteristics of the thermal near field of SiC

using TINS. We find a large variation in SPhP peak shift from ~ 5 up to ~ 50 cm^{-1} . While conventional dipole-dipole coupling can explain some of the shift, it seems insufficient to explain the most extreme spectral redshift. This suggests a modification of the SPhP condition through a previously not considered effective medium change due to the tip proximity to the surface. In addition, we observe an exponential distance dependence as compared to a much steeper scaling as expected and previously observed for the thermal evanescent near field of uncorrelated local emitter [4]. This exponential distance dependence can be explained by spatial coherence arising from the correlation of thermal polarization via the nonlocal nature of the SPhP, despite the excitation through stochastic fluctuations. However, a breakdown of macroscopic electrodynamics for distances shorter than the phonon mean free path is also discussed as a possible alternative [8]. The results highlight scattering and frustration as a sensitive probe of, as well as a means to control, thermal near-field properties.

The thermal excitation of a randomly fluctuating optical polarization and its possible coupling to material-specific resonances determine the spatial and spectral properties of the EM-LDOS, in both the near and the far field. The EM-LDOS $\rho(\vec{r}, \omega)$ is described through the fluctuation-dissipation theorem with material properties entering through the Green's dyadic tensor [2]. To illustrate on-resonance behavior, we consider the limiting case of the quasistatic near-field regime ($z \ll \lambda$), valid in close proximity to the medium with

$$\rho_{\text{evan}}(z, \omega) \simeq \frac{1}{4\pi^2 \omega z^3} \frac{\text{Im}(\epsilon_2)}{|\epsilon_2 + \epsilon_1|^2}, \quad (1)$$

where ϵ_1 and ϵ_2 are the frequency-dependent dielectric functions of the upper and lower half spaces, respectively [9]. As seen from Eq. (1), $\rho_{\text{evan}}(z, \omega)$ is resonantly enhanced via $\text{Im}(\epsilon_2) = 2nk$ (intrinsic resonance), corresponding to a peak in absorption for a weakly dispersive resonance, or for collective excitations when the surface polariton condition is met at $\text{Re}(\epsilon_2) = -\text{Re}(\epsilon_1)$ (extrinsic resonance).

II. EXPERIMENT

The enhanced EM-LDOS of the thermal evanescent near field gives rise to scattering when interacting with a nanoscopic

*Corresponding author: markus.raschke@colorado.edu

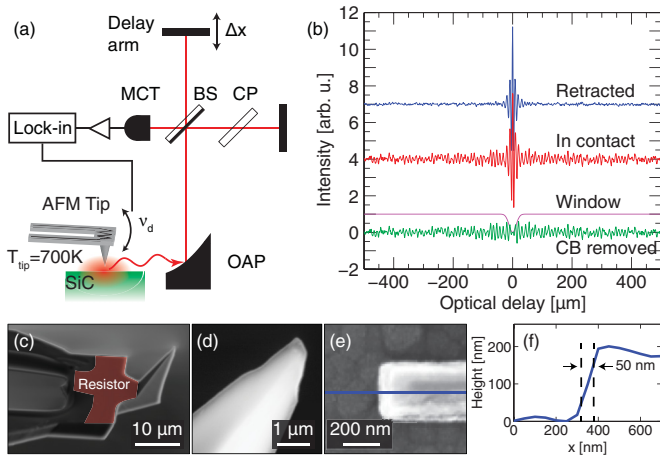


FIG. 1. (Color online) (a) Thermal infrared near-field spectroscopy using heated AFM tips to provide both local excitation and scattering of the thermal near field of the sample, as detected by FTIR spectroscopy. (b) Interferograms with tip retracted (blue curve) and tip in contact with SiC (red curve), and with the center burst removed (green curve) by a window function (magenta curve). Long-range interference in contact (red curve) indicates coherent contribution due to the SPhP resonance. (c),(d) SEM images of thermal cantilever tips. (e) SEM image of test structure with corresponding AFM line trace (f) with apex radius of ~ 50 nm.

tip providing a perturbation for k vectors $\propto 1/r$, with r the tip apex radius. The experimental setup [Fig. 1(a)] is based on an atomic force microscope (AFM, Anasys Instruments) using customized silicon tips with a built-in resistive heater as described previously [4]. Figures 1(c) and 1(d) show scanning electron microscopy (SEM) images of typical cantilever assembly (c) and tip apex region (d). The AFM line trace (f) of a ~ 200 -nm-high test structure (e) allows us to verify a regular tip shape and derive an apex radius of ~ 50 nm. With tip temperatures up to $T_{\text{tip}} \approx 700$ K, this allows for local sample heating up to ~ 550 K while maintaining stable noncontact AFM feedback. Simultaneously, the tip scatters the induced evanescent thermal near field of the sample into detectable far-field radiation. The scattered infrared light is collected with an off-axis parabolic (OAP) mirror, sent through a Michelson-type interferometer with a beam splitter (BS) and a compensation plate (CP), and detected with a mercury-cadmium-telluride (MCT) detector (AG&G, J15D14). The near-field signal is discriminated from the far-field background by lock-in demodulation at the tip-dither frequency ν_d . Spectral information is obtained through Fourier transform infrared (FTIR) spectroscopy. The SiC surface exhibits a strongly dispersive SPhP resonance expected to peak at 948 cm^{-1} at the SiC/air interface.

III. RESULTS

Typical TINS interferograms are shown in Fig. 1(b). With the tip retracted (blue curve), the narrow center burst reflects the large spectral bandwidth and low coherence of the heated tip blackbody spectrum. When near SiC, the tip-scattered interferogram (red) indicates the increased temporal coherence of the quasimonochromatic SPhP resonantly enhanced thermal

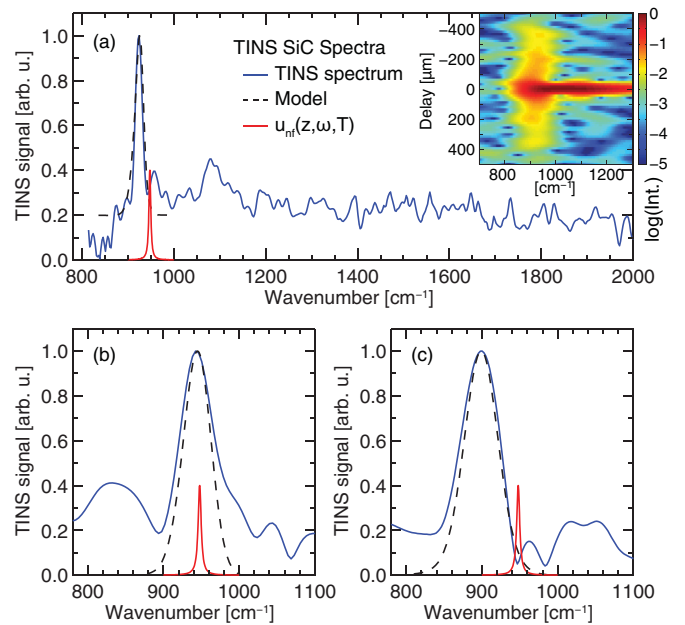


FIG. 2. (Color online) Fourier transformed TINS spectra of SiC (blue curve, with corresponding spectrogram). Fits (black dashed curve) using finite dipole model (a),(b) and effective medium model (c). Calculated spectral energy density $u(100 \text{ nm}, \omega, 300 \text{ K})$ (red curve, arb. units). Spectra are redshifted by about 5 cm^{-1} (b), 25 cm^{-1} (a), and 50 cm^{-1} (c), indicating the high sensitivity of thermal SPhP response to extrinsic effects.

near field. Figure 2(a) shows the corresponding broadband Fourier transform and spectrogram (inset) of the in-contact interferogram from Fig. 1(b). The enhanced emission peak is induced by the SPhP resonance with flat spectral response otherwise. We note that the technique is inherently broadband with no specific resonances associated with material or geometry of the Si tips in the spectral range investigated.

For subsequent data analysis, we first apply a window function [Fig. 1(b), magenta curve] to suppress the center burst of the interferogram [see Fig. 1(b), green curve], which is dominated by the incoherent both near- and far-field off-resonant background. Two additional representative spectra from Fourier transformed (prefiltered) interferograms are shown in Figs. 2(b) and 2(c). For each spectrum shown in Figs. 2(a)–2(c), taken using different tips, the peaked SPhP near-field signal can be seen. It is associated with the spectral energy density of SiC $u(z, \omega, T)$ (red curve, calculated for $z = 100 \text{ nm}$ and $T = 300 \text{ K}$), yet redshifted by varying amounts of 5 cm^{-1} (b), 25 cm^{-1} (a), and 50 cm^{-1} (c).

Corresponding TINS distance dependencies are shown in Fig. 3, with integration on- (a) and off-resonance (b) for few precise measurements using long acquisition times and averaging over several interferograms (red circles), and several measurements with shorter acquisition times (blue circles) [4]. For comparison, measured laser scattering-scanning near-field microscopy (s -SNOM) (CO_2 , $\lambda_{\text{ext}} = 10.8 \mu\text{m}$) distance dependencies using the same tips are shown for different harmonic demodulations (ν_d and $2\nu_d$) exhibiting much stronger near-surface spatial confinement compared to TINS.

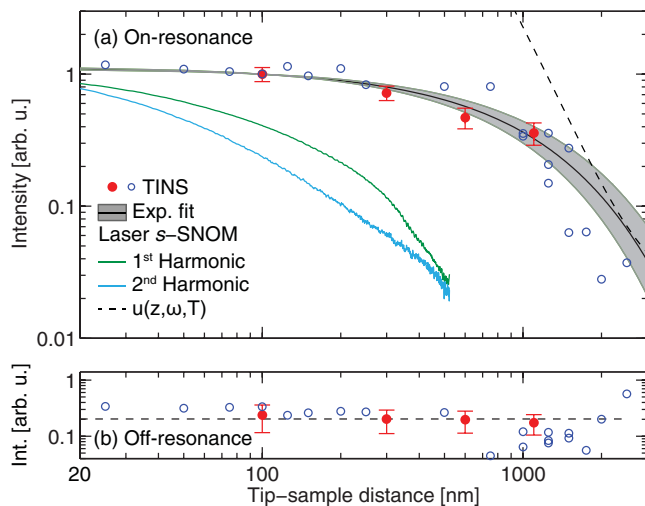


FIG. 3. (Color online) Distance dependence of spectrally integrated TINS measurements of SiC (blue and red circles). On-resonance data (a) show exponential dependence, with a decay constant of $(5.5 \pm 1.0) \times 10^3 \text{ cm}^{-1}$ (black curve; gray region shows uncertainty of fit). Approach curves from laser s -SNOM at the first (green curve) and second (blue curve) cantilever harmonic for comparison. The energy density $u(z, 948 \text{ cm}^{-1}, 300 \text{ K})$ (black dashed curve) shows a $1/z^3$ divergence at short distances.

IV. DISCUSSION

Spectral shifts. In contrast to earlier experiments [4,7], the variable and large spectral shifts of the TINS SPhP peak observed here suggest more complex mechanisms with regards to optical tip-sample coupling and frustration of the evanescent field than previously assumed.

In principle, a few-wave-number redshift can arise from phonon softening when heating the sample [10]. The effect on the dispersion relation for the SPhP condition gives rise to at most $6\text{--}7 \text{ cm}^{-1}$ spectral shifts and a $2\text{--}3 \text{ cm}^{-1}$ increase in linewidth in TINS when heating from 300 K to 550 K. This may account for small shifts such as the 5 cm^{-1} shift in Fig. 2(b) but the larger shifts observed would require higher temperatures than were experimentally accessible ($T > 800 \text{ K}$).

s -SNOM spectra, in general, have been modeled via a modified frequency and tip-sample-distance-dependent tip polarizability [7,11–13]. In the simplest implementation we model TINS as Rayleigh scattering by the tip with scattered power $P_{\text{scat}}(z, \omega, T) = C_{\text{eff}} c u(z, \omega, T)$. $C_{\text{eff}} = k^4 |\alpha_{\text{eff}}|^4 / 6\pi$ is the effective scattering cross section and α_{eff} the effective tip polarizability which depends on optical properties of the tip and sample, as well as tip geometry and position above the surface. The spectral energy density is given by $u(z, \omega, T) = \Theta(\omega, T) \rho(z, \omega)$ with EM-LDOS $\rho(z, \omega)$ and mean thermal photon energy at frequency ω , $\Theta(\omega, T)$ [1,2].

While TINS spectra of local mode molecular resonances can accurately be described with, at most, few cm^{-1} shifts using the point dipole model for α_{eff} [4], it fails for the strongly dispersive and extrinsic SPhP modes [7]. In contrast, the finite dipole model (FDM) [11] simulates α_{eff} via an extended induced charge distribution along the tip shaft over a characteristic length L , with tip radius R , and using a complex

parameter g to describe the effective tip-material response. The parameter g characterizes the ratio of near apex to total charge induced along the tip. The FDM was shown to model SPhP near-field laser s -SNOM spectra of SiC [11,14] and SiO₂ [15] to good agreement.

Figures 2(a) and 2(b) show our FDM fits (black dashed) using $R = 150 \text{ nm}$ and $L = 3 \mu\text{m}$ (a), and $R = 50 \text{ nm}$ and $L = 300 \text{ nm}$ (b), both using $g = 0.8 \exp(i\pi/25)$ and convoluted with an experimental spectral resolution of 11 cm^{-1} (a) and 49 cm^{-1} (b). While the smallest 5 cm^{-1} spectral shift in (b) is readily accommodated using physically meaningful fit parameters, the 25 cm^{-1} shift (a) is already pushing the validity of the quasistatic nature of the model.

A spectral shift as large as 50 cm^{-1} (c) cannot be adequately described using the FDM. This suggests that either the FDM does not capture the essential physics of the tip-sample coupling or additional processes contribute to the spectral shift [13].

Note that larger values of R and L are required to fit the 25 cm^{-1} shifted spectrum [Fig. 2(a)] compared to those used to fit laser-based s -SNOM spectra. For example, in a laser s -SNOM study of SiC with Pt tips a $\sim 25 \text{ cm}^{-1}$ shift was modeled with fit parameters $R \approx 35 \text{ nm}$ and $L = 300 \text{ nm}$ [11]. The larger values of R and L could reflect the differences in the local field distribution induced by the incident laser versus those induced by the thermal near field. Compared to the s -SNOM value of $g = 0.7 \exp(i0.06)$ [11], the larger phase value of g reflects a smaller conductivity of our uncoated Si tips compared to Pt-coated tips.

The thermal near-field interaction may alternatively be described as the tip modifying the SPhP dispersion relation through the near-field interaction when brought close to the surface. This model was used to describe the interaction of the tip with a laser-excited surface plasmon field in a total internal reflection geometry in a photon scanning tunneling microscopy study [16].

To describe the thermal near-field tip-sample interaction resulting in the 50 cm^{-1} redshift in Fig. 2(c), we therefore propose the possibility that the presence of the tip near the surface gives rise to an effective change in dielectric environment $\epsilon_1 = \epsilon_{\text{eff}} \neq 1$, thus altering the SPhP condition in Eq. (1) ($\text{Re}(\epsilon_{\text{eff}}) = -\text{Re}(\epsilon_{\text{SiC}})$) from that of vacuum ($\epsilon_{\text{eff}} = 1$). This method has been applied to s -SNOM studies of nanoantennas [17] and is a valid consideration when an inhomogeneous medium is brought in the near-field region ($z \lesssim \lambda/2\pi \approx 1\text{--}2 \mu\text{m}$) of the surface.

We take the local surrounding within the near-field region of the tip to first approximation as a uniform effective medium of tip material and vacuum given by a linear combination as $\epsilon_{\text{eff}} = (1 - \delta) + \delta \epsilon_{\text{tip}}$ with $0 \leq \delta \leq 1$. Due to the strong dispersion of SiC [Fig. 4(a)], an increasing fraction of Si tip material (b) (dielectric function from Ref. [18]) results in a continuous redshift of the SPhP spectral energy density (c). A modest $\sim 10\%$ Si fraction can already result in an up to 20 cm^{-1} redshift of the spectral energy density (c). With $\delta = 0.35$ we can readily fit the experimental 50 cm^{-1} spectral shift in Fig. 2(c) (black dashed, convoluted with 39 cm^{-1} spectral resolution), even without consideration of additional geometric factors that affect field enhancement, retardation, and scattering. It should be noted that this model breaks down for

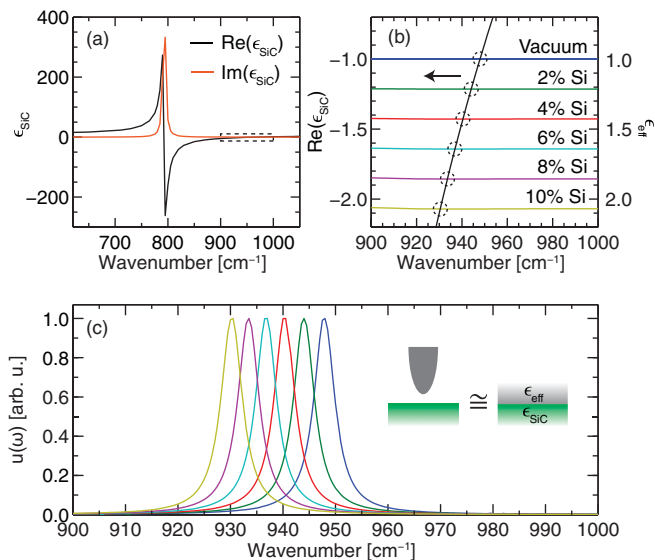


FIG. 4. (Color online) Effective medium theory modifying SPhP resonance condition. (a) $\epsilon(\omega)$ of SiC showing strong dispersion due to the bulk transverse-optical phonon mode at 790 cm^{-1} . (b) Effective dielectric function $\epsilon_{\text{eff}}(\omega)$ for various fractions of Si in the spectral region marked [dashed box in (a)]. The near-field spectral energy density $u(100 \text{ nm}, \omega, 300 \text{ K})$ peaks for $\text{Re}(\epsilon_{\text{eff}}) = -\text{Re}(\epsilon_{\text{SiC}})$ (black dashed circles), with calculated spectral energy density (c) corresponding to the effective medium of (b).

tip materials with, e.g., ϵ_{tip} negative as in the case of metals, where one expects that the local field distribution depends more significantly on exact tip geometry.

While the physical mechanisms of the models of near-field coupling and effective medium change appear different, both show how the tip locally tunes the EM-LDOS, in particular for the case of extrinsic resonances such as SPPs and SPhPs. This is in contrast to weakly dispersive local molecular vibrational resonances as shown previously, e.g., for polytetrafluoroethylene (PTFE) where the peak positions of the C-F molecular resonances are essentially unaffected by the presence of the tip [4]. These results are also consistent with *s*-SNOM spectra where extrinsic or strongly dispersive [19] resonances show significant spectral sensitivity to tip material and geometry [20], while intrinsic resonance peak widths and positions are essentially unaffected [21]. Irrespectively, the results show that the use of TINS for measuring the EM-LDOS of materials with strongly dispersive resonances requires a minimally perturbing probe.

Distance dependence. We now consider the spectrally integrated on- and off-resonance contributions to our TINS signal as a function of distance. In agreement with theory, the experimentally observed [Fig. 3(b)] off-resonance near-field signal is small, and only weakly distance dependent; except for an experimentally unresolved moderate increase expected at very close proximity to the surface [22]. On-resonance (a), over the almost two-orders-of-magnitude distance variation we find an exponential scaling down to the shortest tip-sample distance of $\sim 20 \text{ nm}$. The behavior can be fit (black curve) by $|E_z|^2 \propto e^{-2k_z z}$, with $k_z = (5.5 \pm 1.0) \times 10^3 \text{ cm}^{-1}$. While a pronounced increase in spectral energy density near the surface is expected, for the SPhP resonance, an exponential scaling

of $u(z, 948 \text{ cm}^{-1}, 300 \text{ K})$ starting from the far-field regime ($z > 4 \text{ }\mu\text{m}$) should transition to a much steeper $1/z^3$ distance dependence below $\sim 1 \text{ }\mu\text{m}$ [see Fig. 3(a), black dashed curve] [22,23].

We propose that the observed exponential behavior reflects the spatial coherence and polarization properties of the SiC SPhP thermal near field. It should be noted, however, that the underlying mechanism is different compared to the exponential distance behavior observed in photon tunneling microscopy of laser-excited surface plasmon polaritons, where spatial coherence is expected due to the coherent excitation process [24]. In general, the thermally induced random fluctuations of the transient optical polarization density in the material lead to a spatially incoherent field [23], with a low degree of polarization [25]. It is this incoherent field that underlies the $1/z^3$ -dependent increase in spectral energy density. In the case of SiC, this source polarization couples to the delocalized SPhP excitation, that is spatially coherent in the sample plane, with a coherence length of tens of microns [23]. This gives rise to an exponentially decaying coherent SPhP field confined to within about $\sim 5 \text{ }\mu\text{m}$ of the surface with a decay constant $k_{\text{theory}} = 2.2 \times 10^3 \text{ cm}^{-1}$ as derived from the SPhP dispersion relation for SiC in air.

This spatially coherent and polarized thermal SPhP near field is more efficient to induce a superradiant polarization in the tip due to the finite spatial extent of the apex compared to the incoherent term. The coherent thermal SPhP field can thus be scattered more efficiently compared to a spatially incoherent field from a randomly fluctuating optical polarization, thus giving rise to the experimentally observed exponential distance dependence. This interpretation is supported by the distinct TINS behavior for thermally excited local molecular vibrational resonances. Here the lack of spatial coherence gives rise to a steeper superexponential distance dependence as experimentally demonstrated for PTFE previously [4].

Note that tip heating of the sample is less efficient at larger distances. This explains the shorter experimental decay length with $k_z = (5.5 \pm 1.0) \times 10^3 \text{ cm}^{-1}$, compared to the theoretical value of $k_{\text{theory}} = 2150 \text{ cm}^{-1}$. Nevertheless, the long-range exponential scaling of the TINS data is consistent with the coherent excitation of SPhPs, indicating that the hot tip is effective at heating the sample at least within a distance of $\sim 1 \text{ }\mu\text{m}$ [26]. Alternatively, the effective medium model from above would also predict a shorter decay length with increasing Si content in ϵ_{eff} which follows from the dispersion relation.

While SPhP coherence is a compelling explanation for the exponential distance behavior, an alternative explanation is a possible breakdown of the macroscopic theory used to derive the spectral energy density. The macroscopic theory assumes that the polarization source currents $\mathbf{j}(\mathbf{r}, \omega)$ are δ correlated, $\langle j_\alpha(\mathbf{r}, \omega) j_\beta^*(\mathbf{r}', \omega') \rangle \propto \delta_{\alpha\beta} \delta(\omega - \omega') \delta(\mathbf{r} - \mathbf{r}')$ [8]. A possible breakdown of the macroscopic theory was previously invoked to describe deviations from the theoretically expected distance dependence of heat transfer in scanning thermal microscopy [27]. Here the mean free path of the electrons ($\ell_e \approx 10 \text{ nm}$) sets the scale for the optical current correlations, which need to be compared to the tip length scale which describes the tip-sample interaction. In our experiments, the relevant mean free phonon path, measured to be on the order of $3\text{--}5 \text{ }\mu\text{m}$ [28], is longer

than apex radius or tip dipole extent that follows from FDM to be in the 0.1–1- μm range. A different explanation for the absence of the divergent behavior was proposed in Ref. [29], whereby the heat transfer between metallic plates does not exhibit the divergent distance dependence as attributed to the generation of eddy currents in the medium.

While we believe that these latter two processes are less likely to be the dominant mechanisms responsible for the exponential distance dependence observed, they highlight the unique properties of the thermal near-field and the insight it can provide into the different microscopic processes underlying the optical physics of thermal radiation.

V. CONCLUSION

In summary, the spectral and distance-dependent response of TINS performed on SiC as an example of an extrinsic and strongly momentum-dependent resonance highlights the ability of thermal near-field scattering using TINS to gain

insight into microscopic and coherent processes underlying thermal radiation. In addition, the high spatio-spectral sensitivity of TINS and the unique properties of the thermal near field demonstrate the ability of TINS for testing the limitations of different models used to describe *s*-SNOM in general, which are otherwise difficult to discern. Furthermore, the results indicate how coupled nanostructures or devices can locally modify the EM-LDOS and tune the surface polariton resonance, offering nanoscale control of extrinsic material resonances.

ACKNOWLEDGMENTS

The authors are indebted to Kevin Kjoller and the team from Anasys Instruments for generous support. We also acknowledge valuable discussions with Yannick De Wilde and Jean-Jacques Greffet. Part of this research was supported by the U.S. Department of Energy, Office of Basic Energy Sciences, Division of Materials Sciences and Engineering, under Award No. DE-FG02-12ER46893.

-
- [1] K. Joulain, J.-P. Mulet, F. Marquier, R. Carminati, and J.-J. Greffet, *Surf. Sci. Rep.* **57**, 59 (2005).
 - [2] A. C. Jones, B. T. O’Callahan, H. U. Yang, and M. B. Raschke, *Prog. Surf. Sci.* **88**, 349 (2013).
 - [3] S. Shen, A. Narayanaswamy, and G. Chen, *Nano Lett.* **9**, 2909 (2009).
 - [4] A. Jones and M. Raschke, *Nano Lett.* **12**, 1475 (2012).
 - [5] G. L. Klimchitskaya and V. M. Mostepanenko, *Rev. Mod. Phys.* **81**, 1827 (2009).
 - [6] Y. D. Wilde, F. Formanek, R. Carminati, B. Gralek, P. Lemoine, K. Joulain, J. Mulet, Y. Chen, and J. Greffet, *Nature (London)* **444**, 740 (2006).
 - [7] A. Babuty, K. Joulain, P.-O. Chapuis, J.-J. Greffet, and Y. De Wilde, *Phys. Rev. Lett.* **110**, 146103 (2013).
 - [8] E. Lifshitz and L. Pitaevskii, *Course of Theoretical Physics* (Butterworth-Heinemann, Oxford, 2002), Vol. 9.
 - [9] K. Joulain, R. Carminati, J.-P. Mulet, and J.-J. Greffet, *Phys. Rev. B* **68**, 245405 (2003).
 - [10] D. Olego and M. Cardona, *Phys. Rev. B* **25**, 3889 (1982).
 - [11] A. Cvitkovic, N. Ocelic, and R. Hillenbrand, *Opt. Express* **15**, 8550 (2007).
 - [12] B. Knoll and F. Keilmann, *Opt. Commun.* **182**, 321 (2000).
 - [13] A. S. McLeod, P. Kelly, M. D. Goldflam, Z. Gainsforth, A. J. Westphal, G. Domingues, M. Thiemens, M. M. Fogler, and D. N. Basov, *arXiv:1308.1784v2*.
 - [14] T. Taubner, F. Keilmann, and R. Hillenbrand, *Nano Lett.* **4**, 1669 (2004).
 - [15] S. Amarie and F. Keilmann, *Phys. Rev. B* **83**, 045404 (2011).
 - [16] A. Passian, R. H. Ritchie, A. L. Lereu, T. Thundat, and T. L. Ferrell, *Phys. Rev. B* **71**, 115425 (2005).
 - [17] M. Schnell, A. Garcia-Etxarri, A. J. Huber, K. Crozier, J. Aizpurua, and R. Hillenbrand, *Nat. Photonics* **3**, 287 (2009).
 - [18] E. Palik (ed.), *Handbook of Optical Constants of Solids* (Academic Press, San Diego, 1985), Vol. 1.
 - [19] I. M. Craig, M. S. Taubman, A. S. Lea, M. C. Phillips, E. E. Josberger, and M. B. Raschke, *Opt. Express* **21**, 30401 (2013).
 - [20] A. Garcia-Etxarri, I. Romero, F. J. Garcia de Abajo, R. Hillenbrand, and J. Aizpurua, *Phys. Rev. B* **79**, 125439 (2009).
 - [21] A. A. Goyyadinov, I. Amenabar, F. Huth, P. S. Carney, and R. Hillenbrand, *J. Phys. Chem. Lett.* **4**, 1526 (2013).
 - [22] C. Henkel, K. Joulain, R. Carminati, and J.-J. Greffet, *Opt. Commun.* **186**, 57 (2000).
 - [23] R. Carminati and J.-J. Greffet, *Phys. Rev. Lett.* **82**, 1660 (1999).
 - [24] M. Ohtsu, *J. Lightwave Technol.* **13**, 1200 (1995).
 - [25] T. Setälä, M. Kaivola, and A. T. Friberg, *Phys. Rev. Lett.* **88**, 123902 (2002).
 - [26] Thermal conduction between a macroscopic cantilever with a large aspect ratio and a short tip provides efficient heating through ballistic heat thermal air conduction. Surface melting of polycarbonate samples have verified local heating up to ~ 550 K.
 - [27] A. Kittel, W. Müller-Hirsch, J. Parisi, S.-A. Biehs, D. Reddig, and M. Holthaus, *Phys. Rev. Lett.* **95**, 224301 (2005).
 - [28] J. Freedman, J. Leach, E. Preble, Z. Sitar, R. Davis, and J. Malen, *Sci. Rep.* **3**, 2963 (2013).
 - [29] P.-O. Chapuis, S. Volz, C. Henkel, K. Joulain, and J.-J. Greffet, *Phys. Rev. B* **77**, 035431 (2008).